IEEE Access
Multidisciplinary | Rapid Review | Open Access Journal

Received August 18, 2021, accepted September 17, 2021, date of publication September 23, 2021, date of current version October 1, 2021.

Digital Object Identifier 10.1109/ACCESS.2021.3115149

The Synchronization Behaviors of Memristive Synapse-Coupled Fractional-Order Neuronal Networks

YANG XIN[1] AND ZHANG GUANGJUN[2]
[1]Aeronautics Engineering College, Air Force Engineering University, Xi'an 710038, China
[2]Department of Basic Sciences, Air Force Engineering University, Xi'an 710058, China
Corresponding author: Zhang Guangjun (1418008562@qq.com)

ABSTRACT The synchronization behaviors of memristive synapse-coupled fractional-order neuronal networks are investigated in this paper. Based on the integer-order memristive synapse-coupled neuronal network, a fractional-order model is proposed, and a ring network composed of fractional-order memristive synapse-coupled neuronal subnetworks is constructed. Then, the synchronization behaviors of two fractional-order memristive synapse-coupled neurons and the ring fractional-order memristive synapse-coupled neuronal network are discussed numerically. These research results suggest several novel phenomena and allow several conclusions to be drawn. For the two coupled neurons, different fractional-orders can change the threshold of memristive synapse parameter k_1 when the two neurons are in perfect synchronization. The synchronization transitions are affected by the fractional-order and memristive synapse. Different from the integer-order model, perfect synchronization can occur before phase synchronization for some fractional-orders. Under a certain external current intensity, the transition between periodic synchronization and chaotic synchronization occurs as the fractional-order changes. The chaotic synchronization range is larger because of the memristive synapse. For the ring neuronal network coupled subnetworks, the results illustrate that the collective behaviors including incoherent, coherent, and chimera states can be induced by the fractional-order. In addition, the network's synchronization degree is influenced by the fractional-order. The synchronization transition of the neuronal network also occurs with changes in the fractional-order.

INDEX TERMS Fractional-order neuronal models, neuronal network, memristive synapse, synchronization transition, chimera state.

I. INTRODUCTION

The firing behaviors of neurons are nonlinear processes. Neurons have been modeled and analyzed from a large amount of experimental data, and the results show that the firing of neurons constitutes a complex nonlinear dynamical system. In 1952, Hodgkin and Huxley used equivalent circuits and large amounts of data form experiments to model and analyze the data and constructed the Hodgkin-Huxley (HH) neuron model through a theoretical derivation [1]. In 1961, FitzHugh simplified the variables in the HH model, and constructed a low-dimensional model, the two-dimensional FitzHugh-Nagumo (FHN) model [2]. Morris and Lecar summarized the new neuron model (Morris-Lecar (ML) model), which is a further simplification of the HH model, from experimental data of arctic goose muscle fibers. In 1982, based on data of a voltage clamp experiment of snail nerve cells, Hindmarsh and Rose proposed the Hindmarsh-Rose (HR) model [3]. Synchronization is an important phenomenon in neuronal systems and an important operational mechanism of the brain. A number of researchers have used the coupled neuronal model to try to explain some of the synchronization phenomena observed in experiments. Studying the motor mechanism of the neuronal dynamical system helps understand relevant phenomena in the brain, and contributes to the development of artificial intelligence.

A large number of studies have investigated the synchronization and synchronization transition of neuronal networks [4]–[15]. The relevant literature shows that the main factors affecting the synchronization of coupled neuronal

The associate editor coordinating the review of this manuscript and approving it for publication was Bing Li.

networks are the network topology [4]–[8], time delay in the network [9], [10], coupling strength [11]–[14], and multilayer network structure [15], etc. Recently, researchers have found that the electrical activity of neurons may be affected by electromagnetic fields, and thus, electromagnetic fields can be detected by the neuronal system [16], [17]. Memristors controlled by magnetic fluxes can be treated as coupled synapses between neuronal cells. Some studies investigated the chaos and period of a Hopfield network coupled with memristive synapses [18,19] and the rich dynamic behaviors of memristive synapse-coupled neuronal networks [20]–[22]. By adjusting the relevant parameters, different firing models arise, increasing the synchronization efficiency in a memristive synapse-coupled neuronal network [20]. Different synchronization behaviors are observed when the neuron initial states change [22].

The above studies investigated integer-order neuronal networks. Fractional-order neuronal networks can give a more complete picture of nature than their integer-order counterparts. In the past, scholars have conducted many studies on fractional-order dynamical systems and applied them in many fields, such as financial systems [23], biomedical systems [24], [25], and the spread of infectious diseases [26]. [27] proposed a new numerical method based on two-step Lagrange polynomial interpolation to obtain numerical simulations and adaptive anti-synchronization schemes for two fractional conformable attractors of variable order. In terms of fractional-order neuronal models, single fractional-order HR neuronal models [28] was investigated, and the transitions of chaotic firing to periodical firing, spike firing and bursting firing were observed. Two coupled neurons were found to achieve complete synchronization through a designed controller [29]–[31]. Two coupled neurons with magnetic flux can achieve perfect synchronization by adaptive controlling. Coupled fractional-order HR neuronal models without memristive synapse-coupling was investigated in [32]; it was observed that different fractional-orders can induce different synchronization models. The above references illustrate that the fractional-order is an important parameter that can induce rich dynamical behaviors. Few studies have been performed on the synchronization and synchronization transition of coupled fractional-order neuronal networks. Complex synchronization transition and emergence phenomena occur when fractional-order neurons are coupled with memristive synapses, but there is no literature on this topic. The phenomenon of chimera states can describe the related degree of neurons in the network [33], and this phenomenon is widespread in neuronal networks [34]–[38], such as nonlocally and globally coupled time-delay Mackey-Glass oscillators [35], and subnetworks distributed in different regions of neuronal networks [38]. The chimera states, coherent states and incoherent states could be relevant for brain dynamics.

Many studies adopt the predict-corrector method [39], [40] to study fractional-order systems. The predict-corrector method has a high accuracy but a large computational cost. The Adomian decomposition method (ADM) used in this paper also has a high computational cost, but this cost is smaller than that of the predict-corrector method [41].

This paper is organized as follows: First, a memristive synapse-coupled fractional-order HR neuronal network model is proposed, and a ring network is constructed by subnetworks. Then, the synchronization behavior and synchronization transitions of coupled neurons under the influence of fractional-order and memristive synapse-coupling are investigated by numerical simulation. Finally, the synchronization transitions and chimera states of the ring network with fractional-order variation are discussed.

II. MODEL DESCRIPTION

There are many definitions of fractional derivatives, and in practice, three definitions are most frequently used: the Grunwald-Letnikov, Riemann-Liouville and Caputo derivatives. According to [25], under some conditions, these three definitions are equivalent and can be inter-translated. The Caputo derivative makes the Laplace transform more concise, and the physical meaning of the initial condition in the Caputo derivative is clear, so it is simpler to solve the fractional-order derivative. Similar to most studies, the Caputo derivative is adopted in this paper.

Definition 1: The Caputo derivative of the function $f(x)$ is defined as

$$ {}_0^C D_t^q f(x) = \frac{1}{\Gamma(n-q)} \int_0^t \frac{f^{(n)}(\tau)}{(t-\tau)^{q-n+1}} d\tau $$

where $n-1 < q < n$ and $\Gamma(\bullet)$ is the gamma function, which is defined as

$$ \Gamma(z) = \int_0^\infty t^{z-1} e^{-1} dt $$

In particular, when $0 < q < 1$,

$$ {}_0^C D_t^q f(x) = \frac{1}{\Gamma(1-q)} \int_0^t \frac{f'(\tau)}{(t-\tau)^q} d\tau $$

To analyze the dynamic behavior of the memristive synapse-coupled fractional-order neuronal network, the fractional-order HR model is adopted for the single neuronal model. The fractional-order HR model is described as follows [32]:

$$ \begin{cases} D_t^q x = y - ax^3 + bx^2 - z + I \\ D_t^q y = c - dx^2 - y \\ D_t^q z = r\left[s(x - \bar{x}) - z\right] \end{cases} \tag{1} $$

where x is the membrane action potential, y is a recovery variable, z is a slow adaptation current, D_t^q is the differential operator defined by Caputo, and q is the fractional-order. I is the external stimulus current. In this paper, other constants are fixed as $a = 1, b = 3, c = 1, d = 5, r = 0.006, \bar{x} = -1.56$ and $s = 4$.

In this paper, from the integer-order memristive synapse-coupled neuronal network proposed in [21] and the

fractional-order HR model proposed in [28], the memristive synapse-coupled fractional-order neuronal network constructed by two neurons can be described as follows:

$$\begin{cases} D_t^q x_1 = y_1 - ax_1^3 + bx_1^2 - z_1 + I + k_1\omega(\varphi)(x_2 - x_1) \\ D_t^q y_1 = c - dx_1^2 - y_1 \\ D_t^q z_1 = r[s(x_1 - \bar{x}) - z_1] \\ D_t^q x_2 = y_2 - ax_2^3 + bx_2^2 - z_2 + I + k_1\omega(\varphi)(x_1 - x_2) \\ D_t^q y_2 = c - dx_2^2 - y_2 \\ D_t^q z_2 = r[s(x_2 - \bar{x}) - z_2] \\ D_t^q \varphi = x_1 - x_2 - k_2\varphi \end{cases} \quad (2)$$

The cubic flux-controlled memristor model $\omega(\varphi) = dq(\varphi)/d\varphi = \alpha + 3\beta\varphi^2$ is introduced in this model [17], [18], [21], [31], [32]. Here, $\omega(\varphi)$ and φ represent memductance and magnetic flux, respectively. The parameters α and β describe the memory-conductance, and they vary with the environment and their own conditions. The two fractional-order neurons are coupled with a memristive synapse, as shown in Fig. 1. In this paper, the parameters are set as $\alpha = 0.2$, $\beta = 0.02$, and $k_2 = 0.2$.

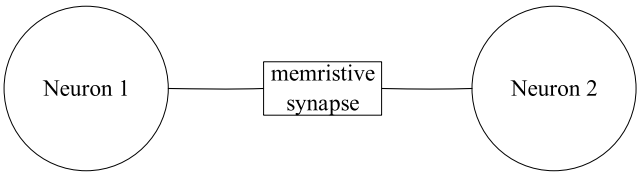

FIGURE 1. Diagram of two fractional-order neurons coupled with a memristive synapse.

A ring network is constructed by some subnetworks that are the abovementioned memristor synapse-coupled networks, and the ring networks involve N subnetworks. Here, $[x_{1i}, y_{1i}, z_{1i}, x_{2i}, y_{2i}, z_{2i}, \varphi_i]$ are the variables of the ith subnetwork. The model can be described as (3), shown at the bottom of the page, where $i = 1, 2, \ldots, N$ and where D is the coupling strength of the ring network. Each memristor synapse-coupled neuronal subnetwork is symmetrically coupled to its P nearest neighbors. In our simulation, N is set as 100, and P is set as 20. The ring connection pattern is presented in Fig. 2. Note that $j = -m$, $(m = 1, 2, \ldots)$ implies that sub-network j is coupled with subnetwork $(101 - m)$.

III. TWO FRACTIONAL-ORDER NEURONS COUPLED WITH A MEMRISTIVE SYNAPSE

As the simplest neuronal network, the synchronization behaviors of two coupled fractional-order neuronal models is researched first.

Before considering the diverse synchronization behaviors, we prove the synchronization of two coupled fractional-order neuronal models theoretically. The Mittag-Leffler function is defined by

$$E_{\alpha,\beta}(z) := \sum_{i=0}^{\infty} \frac{z^i}{\Gamma(\alpha i + \beta)}$$

Lemma 1 [42]: Let $x(t) \in C^m$ be a real continuous and differentiable vector function. Then for all $t \geq t_0$ and $0 < q < 1$, the following inequality holds:

$$D^q\left(x^H(t)Px(t)\right) \leq x^H(t)P\left(D^q x(t)\right) + \left(D^q x^H(t)\right)Px(t)$$

Lemma 2 [43]: Let $V(t)$ be a continuous function on $[t_0, +\infty)$ that satisfies

$$D^q V(t) \leq \theta V(t),$$

where $0 < q < 1$ and θ are constants, then

$$V(t) \leq V(t_0)E_\alpha\left(\theta(t - t_0)^\alpha\right)$$

Lemma 3 [44]: For $0 < q < 1, t \in \mathbb{R}, t > 0$, we have

$$\lim_{t\to\infty} E_q(t) \leq \lim_{t\to\infty} \frac{1}{q} e^{t^{\frac{1}{q}}}$$

Let $\boldsymbol{X} = (x_1, y_1, z_1)$, $\boldsymbol{Y} = (x_2, y_2, z_2)$, and $\boldsymbol{K}_1 = (k_1, 0, 0)$. The error system is $\boldsymbol{e} = \boldsymbol{X} - \boldsymbol{Y}$. According to (2), the error system can be described as

$$\boldsymbol{e} = f(\boldsymbol{X}) - f(\boldsymbol{Y}) - 2\boldsymbol{K}_1\omega(\varphi)(\boldsymbol{X} - \boldsymbol{Y})$$

where

$$f(\boldsymbol{X}) = \begin{bmatrix} y_1 - ax_1^3 + bx_1^2 - z_1 + I_{exc} + k_1\omega(\varphi)(x_2 - x_1) \\ c - dx_1^2 - y_1 \\ r[s(x_1 - \bar{x}) - z_1] \end{bmatrix}$$

$$f(\boldsymbol{Y}) = \begin{bmatrix} y_2 - ax_2^3 + bx_2^2 - z_2 + I_{exc} + k_1\omega(\varphi)(x_1 - x_2) \\ c - dx_2^2 - y_2 \\ r[s(x_2 - \bar{x}) - z_2] \end{bmatrix}$$

$$\begin{cases} D_t^q x_{1i} = y_{1i} - ax_{1i}^3 + bx_{1i}^2 - z_{1i} + I + k_1\omega(\varphi)(x_{2i} - x_{1i}) + \dfrac{D}{2P}\displaystyle\sum_{j=i-p}^{i+p}(x_{1j} - x_{1i}) \\ D_t^q y_{1i} = c - dx_{1i}^2 - y_{1i} \\ D_t^q z_{1i} = r[s(x_{1i} - \bar{x}) - z_{1i}] \\ D_t^q x_{2i} = y_{2i} - ax_{2i}^3 + bx_{2i}^2 - z_{2i} + I + k_1\omega(\varphi)(x_{1i} - x_{2i}) \\ D_t^q y_{2i} = c - dx_{2i}^2 - y_{2i} \\ D_t^q z_{2i} = r[s(x_{2i} - \bar{x}) - z_{2i}] \\ D_t^q \varphi_i = x_{1i} - x_{2i} - k_2\varphi_i \end{cases} \quad (3)$$

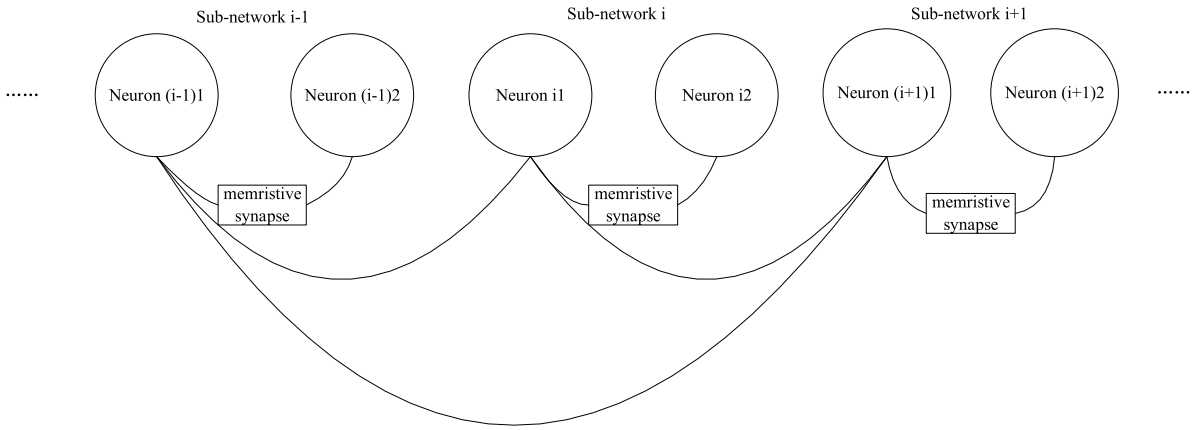

FIGURE 2. Structure of the ring network.

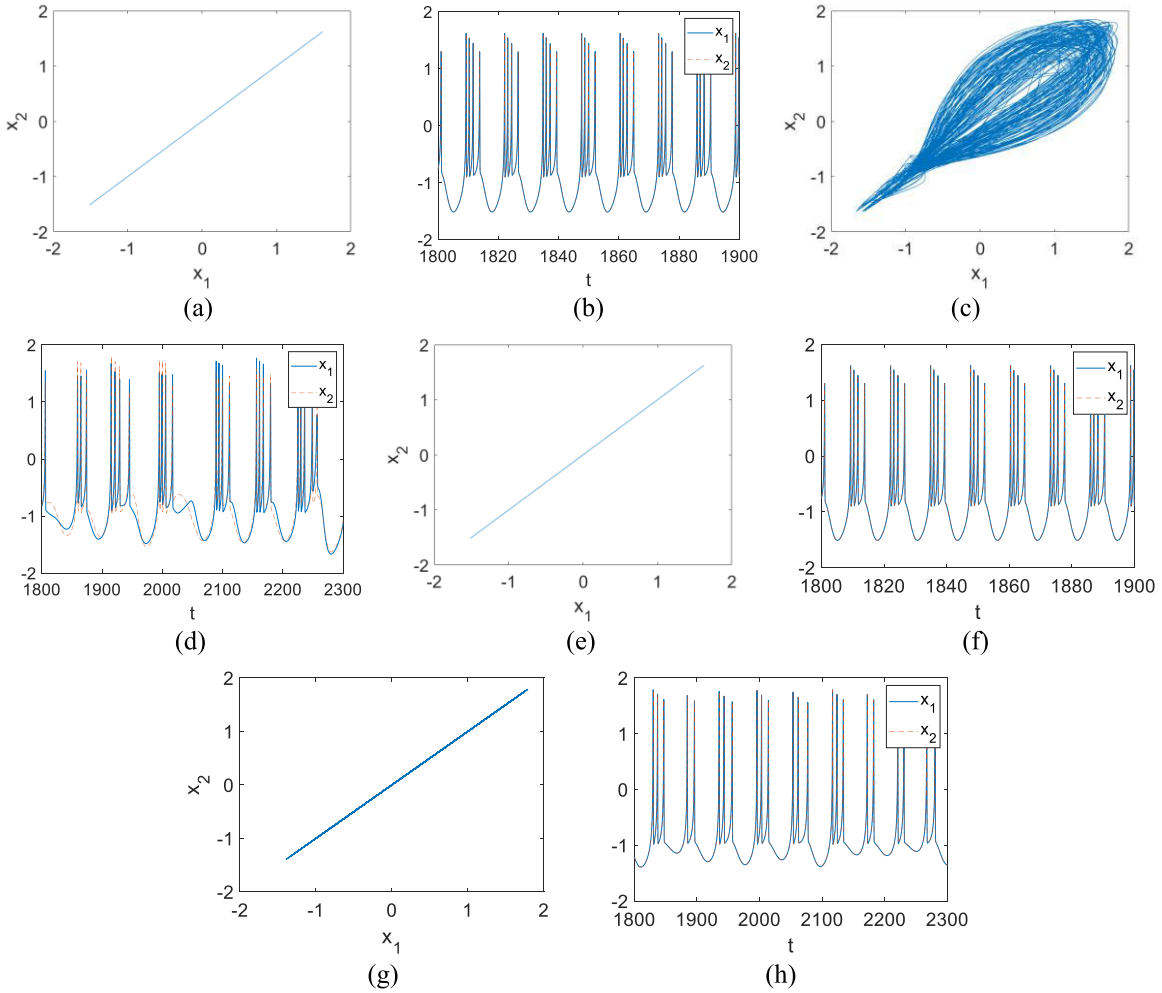

FIGURE 3. Phase diagrams of (x_1, x_2) for (a) $q = 0.56, k_1 = 1.7$, (c) $q = 0.9, k_1 = 1.7$, (e) $q = 0.56, k_1 = 2$, and (g) $q = 0.9, k_1 = 2$. Corresponding time series of x for (b) $q = 0.56, k_1 = 1.7$, (d) $q = 0.9, k_1 = 1.7$, (f) $q = 0.56, k_1 = 2$, and (h) $q = 0.9, k_1 = 2$.

Theorem 1: $f(\bullet)$ satisfy the Lipschitz condition $\|f(X) - f(Y)\| \leq L\|X - Y\|$ [20]; if

$$L - 2k_1\omega(\varphi) < 0,$$

then the two neuronal models can achieve globally exponentially synchronization.

Proof: Construct the Lyapunov function as $V = e^T e$. From **Lemma 1**, the Lyapunov function can be reduced to

$$\begin{aligned} D^q V(t) &\leq \boldsymbol{e}^T D^q \boldsymbol{e} + \left(D^q \boldsymbol{e}^T\right)\boldsymbol{e} \\ &= \boldsymbol{e}^T \left(f(\boldsymbol{X}) - f(\boldsymbol{Y}) - 2\boldsymbol{K}_1\omega(\varphi)(\boldsymbol{X} - \boldsymbol{Y})\right) \end{aligned}$$

$$
\begin{aligned}
&+ (f(\boldsymbol{X}) - f(\boldsymbol{Y}) - 2\boldsymbol{K}_1\omega(\varphi)(\boldsymbol{X}-\boldsymbol{Y}))^T \boldsymbol{e} \\
&= \boldsymbol{e}^T (f(\boldsymbol{X}) - f(\boldsymbol{Y})) - 2\boldsymbol{e}^T \boldsymbol{K}_1\omega(\varphi)(\boldsymbol{X}-\boldsymbol{Y}) \\
&\quad + (f(\boldsymbol{X}) - f(\boldsymbol{Y}))^T \boldsymbol{e} - 2(\boldsymbol{K}_1\omega(\varphi)(\boldsymbol{X}-\boldsymbol{Y}))^T \boldsymbol{e} \\
&\le \boldsymbol{e}^T (L\|\boldsymbol{X}-\boldsymbol{Y}\|) - 2k_1\omega(\varphi)\boldsymbol{e}^T\boldsymbol{e} \\
&\quad + (L\|\boldsymbol{X}-\boldsymbol{Y}\|)^T e - 2k_1\omega(\varphi)\boldsymbol{e}^T\boldsymbol{e} \\
&\le 2L\|\boldsymbol{e}\|^2 - 4k_1\omega(\varphi)\|\boldsymbol{e}\|^2 \\
&= (2L - 4k_1\omega(\varphi))V(t)
\end{aligned}
$$

From **Lemma 2**, $V(t) \le V(t_0)\, E_q((2L-4k_1\omega(\varphi))(t-t_0)^q)$, according to **Lemma 3**,

$$
\lim_{t\to\infty} E_q\left((2L-4k_1\omega(\varphi))(t-t_0)^q\right) \le \lim_{t\to\infty} \frac{1}{q} e^{(t-t_0)(2L-4k_1\omega(\varphi))^{\frac{1}{q}}}
$$

Thus, $V(t) \le V(t_0)\frac{1}{q}e^{(t-t_0)(2L-4k_1\omega(\varphi))^{\frac{1}{q}}}$ as $t \to \infty$. When $L - 2k_1\omega(\varphi) < 0$, we can conclude that the two neuronal models can be globally exponentially synchronized when under the appropriate k_1. This completes the proof.

The parameter I is now set as $I = 3$. Numerical simulation is provided for model (2) by utilizing the ADM method. Fig. 3 displays the phase diagrams, and the corresponding time series of x. As shown in Fig 3(a)(b), when $q = 0.56, k_1 = 1.7$, the system is in perfect synchronization which indicates that variable x_1 is the same as x_2 over sufficient time. The system is in imperfect synchronization when $q = 0.9, k_1 = 1.7$(Fig. 3(c)(d)). As shown in Fig. 3(e)-(h), when $q = 0.56, k_1 = 2$ and $q = 0.9, k_1 = 2$, the system is in perfect synchronization. Through the above analysis, different synchronization behaviors arise when the fractional-order and k_1 change.

To further illustrate the effects of the fractional-order and k_1 on the synchronization of the memristive synapse-coupled neuron, in this paper, the similarity function [31] is introduced to measure the synchronization degree of the system. This function can be described as follows:

$$
S = \left[\frac{\langle (x_1(t) - x_2(t))^2 \rangle}{\left(\langle x_1^2(t)\rangle \langle x_2^2(t)\rangle\right)^{\frac{1}{2}}}\right]^{\frac{1}{2}} \tag{4}
$$

where $\langle \bullet \rangle$ stands for the temporal average. Perfect synchronization can be observed when S is equal to 0, and the greater S is, the worse the synchronization.

When the system is not in perfect synchronization, it may be in phase synchronization. The phase information can be calculated by detecting the time of sampled time series $(t_1, t_2, \ldots, t_n)$ across the Poincare section, and the phase is calculated by [40]

$$
\varphi = 2\pi \frac{t - t_i}{t_{i+1} - t_i} + 2\pi i, \quad t_i < t < t_{i+1} \tag{5}
$$

The phase difference between two neurons is defined by

$$
\Delta\varphi = |\varphi_1 - \varphi_2|
$$

When the phase difference is approximately 0, the coupled neuronal models are in phase synchronization.

To analyze the different synchronization behaviors, the bursting phase difference is introduced in this paper. The phase information can be calculated by detecting the time of variable z time series $(t_1, t_2, \ldots, t_n)$ across the Poincare section, and the bursting phase is calculated by:

$$
\varphi_z = 2\pi \frac{t - t_i}{t_{i+1} - t_i} + 2\pi i, \quad t_i < t < t_{i+1} \tag{6}
$$

The bursting phase difference is defined as:

$$
\Delta\varphi_z = |\varphi_{z1} - \varphi_{z2}|
$$

When the bursting phase difference is approximately 0, the coupled neuronal models are in bursting phase synchronization.

A. SYNCHRONIZATION BEHAVIORS UNDER DIFFERENT FRACTIONAL-ORDERS AND MEMRISTOR SYNAPSES

When the fractional-order q and parameter k_1 are varied in the ranges $[0.55, 1]$ and $[1, 2.5]$, respectively, the similarity function is shown in Fig. 4, where the blue region with S equal to 0 denotes that the system is in perfect synchronization. Regions of other colors imply that the system is not in perfect synchronization. At some fractional-orders, the synchronization is enhanced when k_1 increases. The threshold of k_1 when the system is in perfect synchronization changes greatly with a change in the fractional-order. When $q = 0.55$, the system is in perfect synchronization when $k_1 > 1.42$, but when $q = 0.7$, the system is in perfect synchronization when $k_1 > 2.2$.

To more intuitively observe the effect of the fractional-order on the system synchronization, the thresholds of k_1 for each fractional-order when the system is in perfect synchronization are plotted in Fig. 5. When $0.55 < q < 0.73$, the threshold of k_1 increases with increasing fractional-order. When $0.73 < q < 1$, the threshold first decreases and then fluctuates in the vicinity of 2 with increasing fractional-order. Therefore, when $0.73 < q < 1$, there is not much change in the threshold.

B. SYNCHRONIZATION TRANSITIONS INDUCED BY DIFFERENT FRACTIONAL-ORDERS AND MEMRISTOR SYNAPSES

Fig. 5 shows that the threshold changes greatly from 1.48 to 1.7 near $q = 0.6$. As shown in Fig. 4, near 0.6, there is a smaller k_1 that makes the system be in perfect synchronization, but a larger k_1 does not cause the system to be in perfect synchronization. Fig. 6 shows the curve of $S \sim k_1$ when q is 0.604. The system is in perfect synchronization when $1.55 < k_1 < 1.6$, but when $1.6 < k_1 < 1.8$, the synchronization degree is weakened. The phase diagrams of (x_1, x_2) are shown in Fig. 7 when $k_1 = 1.3, 1.58, 1.7, 2.0$. These phase diagrams show the transitions of the system synchronization with k_1. When $k_1 = 1.3, 1.7$, the corresponding time series of x are shown in Fig. 7(e)(f), indicating that the system is in imperfect synchronization.

As shown in Fig. 8(a)(b), the two neurons are not in phase synchronization when $k_1 = 1.3$ because the phase

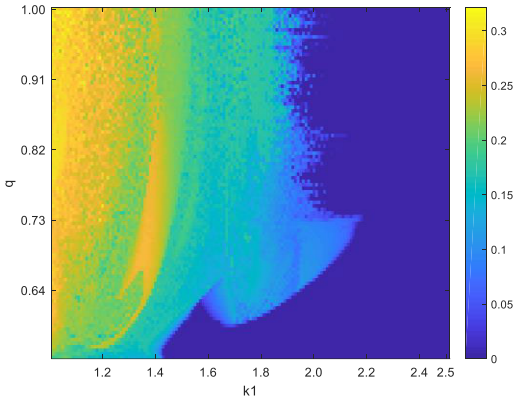

FIGURE 4. Distribution of the similarity function in the $q - k_1$ plane.

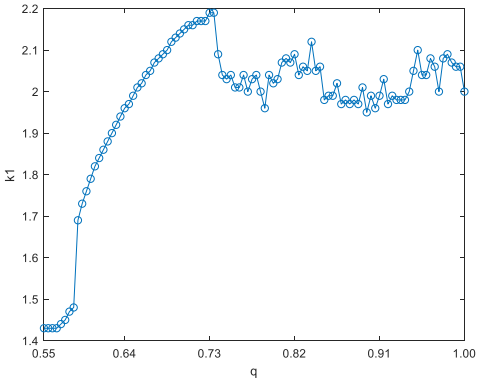

FIGURE 5. Curve of $k_{1cr} \sim q$.

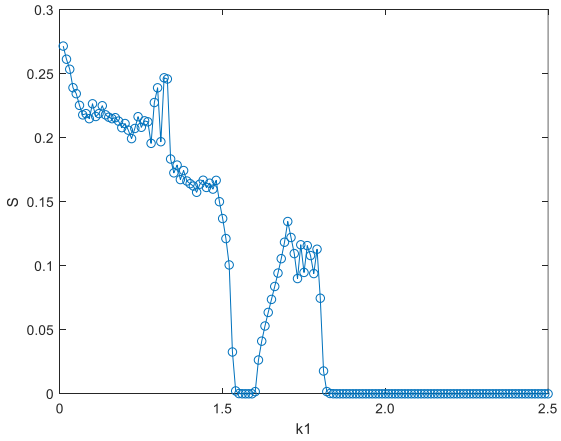

FIGURE 6. Curve of $S \sim k_1$ for $q = 0.604$.

difference is large, but the neurons can reach bursting phase synchronization because the bursting phase difference is small (approximately 0). From Fig. 8(c), it is concluded that the neurons are in phase synchronization when $k_1 = 1.7$. The synchronization transition is as follows: asynchronization → bursting phase synchronization → perfect synchronization → phase synchronization → perfect synchronization.

From the above analysis, it can be found that the effect of the fractional-order on the memristive synapse-coupled neuronal network is complex. Under different fractional-orders, the synchronization behaviors of the system with changing k_1 are different. The system does not strictly follow the transition from phase synchronization to perfect synchronization; perfect synchronization occurs before phase synchronization. In [21], for an integer-order model, the synchronization degree is strengthened with increasing k_1, but in this paper, an exception can be found when the fractional-order is in the range [0.59, 0.64].

C. TRANSITION BETWEEN PERFECT CHAOTIC SYNCHRONIZATION AND PERFECT PERIODIC SYNCHRONIZATION INDUCED BY THE FRACTIONAL-ORDER

As shown in Fig. 3, when $q = 0.56$ and $q = 0.9$, the system is in perfect synchronization, but the firing modes are different. When $q = 0.56$, the neurons display periodic bursting firing. When $q = 0.9$, the neurons display chaotic firing. In Fig. 9, the left and middle panels display the phase diagrams of $(z_{1,2}, x_{1,2})$ and $(x_{1,2}, y_{1,2})$, respectively, when $I = 3, k_1 = 0.3$, and the right panel displays the bifurcation for the integer spike interval (ISI) in one neuron with a bifurcation parameter of k_1 when $I = 3$. As shown in Fig. 9(a)(b)(c), when $q = 0.56$, the neurons display periodic-4 bursting. When $q = 0.9$, the neurons display chaotic firing, as shown in Fig. 9(d)(e)(f).

As shown in Fig. 4, when $k_1 = 2.5$, the system is in perfect synchronization, and when $k_1 = 3$, the system is still in perfect synchronization. The bifurcation for ISI in one neuron to fractional-order q when $k_1 = 3$ is shown in Fig. 10. From Fig. 10, when $0.55 < q < 0.73$, the neurons display periodic bursting, so the system is in perfect periodic synchronization. When $0.73 < q < 1$, the neurons display chaotic bursting, so the system is in perfect chaotic synchronization. The perfect chaotic synchronization range is more extensive than that without memristive synapse-coupling [31]. When the fractional-order changes, a transition between periodic synchronization (periodic-4 synchronization) and perfect chaotic synchronization can be observed. The above analysis shows that the fractional-order not only changes the threshold of k_1 when the system reaches synchronization but also changes the synchronization mode. Memristive synapse-coupling can extend the chaotic synchronization range. Compared with [21], the integer-order coupled neurons are in chaotic synchronization only when the external stimulation current $I = 3$, but the fractional-order coupled neurons can be in periodic synchronization when the fractional-order lies within [0.55, 0.73].

The above discussion concerns the influences of parameter k_1 on the synchronization and the phenomenon of synchronization transition induced by the fractional-order when the external stimulation current $I = 3$. Fig. 11 shows the relevant images when I takes different values and k_1 is set as 3. When $I = 3.5$ and the system is in perfect periodic-5 bursting synchronization and perfect spiking synchronization, the phase diagrams of $q = 0.56$ and $q = 0.9$ are

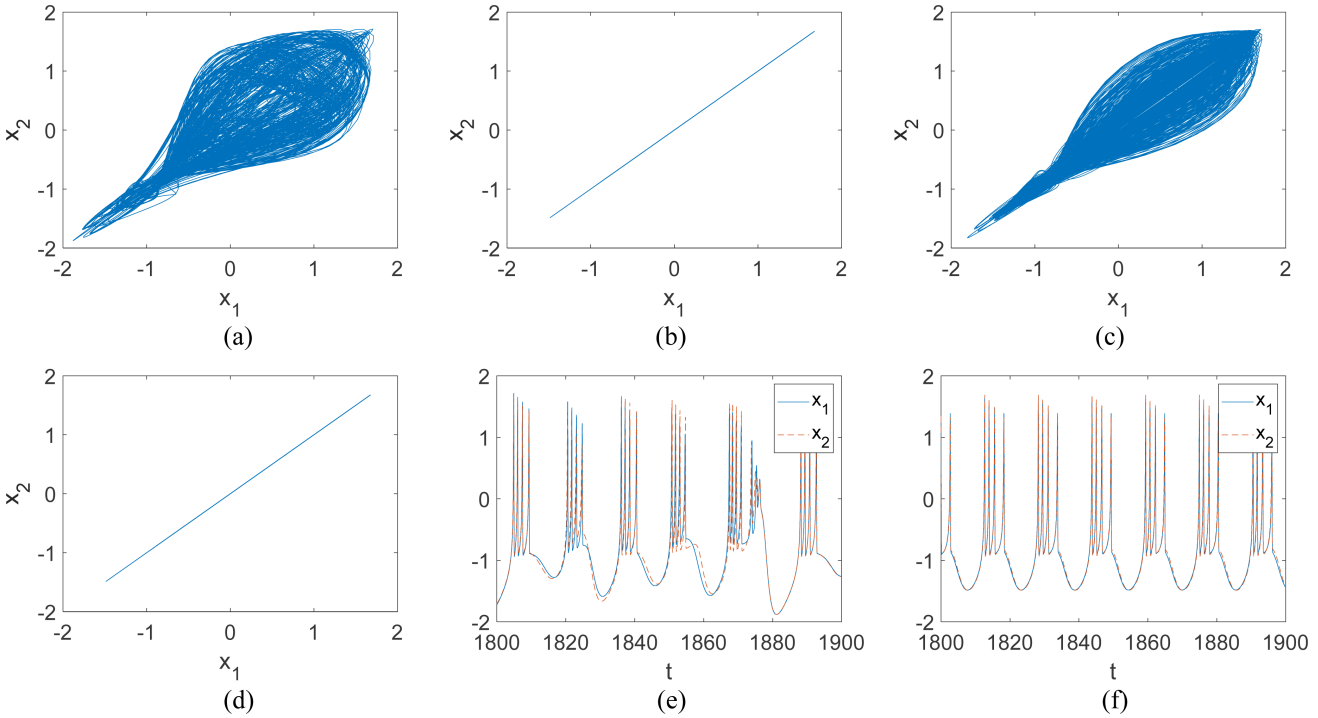

FIGURE 7. Phase diagrams of (x_1, x_2) for $q = 0.6$ (a) $k_1 = 1.3$, (c) $k_1 = 1.58$, (e) $k_1 = 1.7$, and (g) $k_1 = 2$. Corresponding time series of x for (e) $k_1 = 1.3$, and (f) $k_1 = 1.7$.

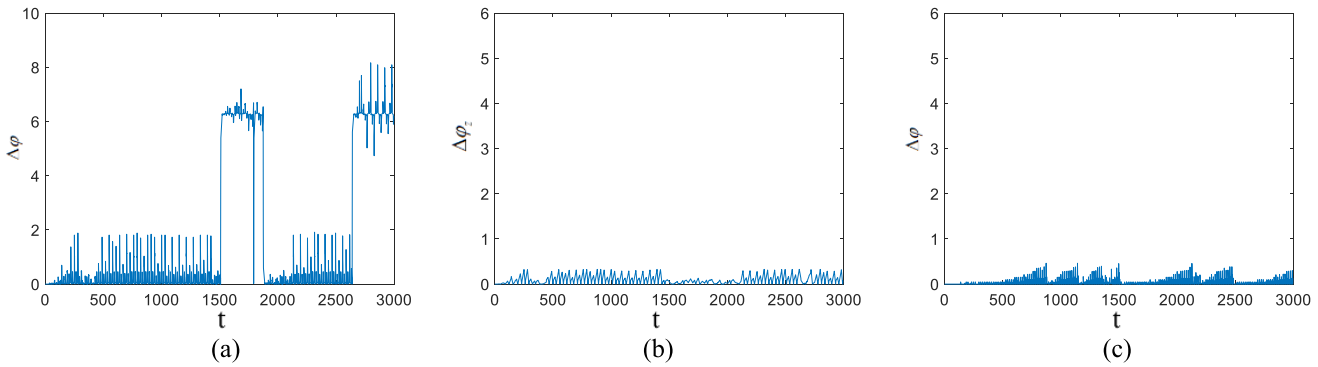

FIGURE 8. Phase difference variations with time: (a) $k_1 = 1.3$, and (c) $k_1 = 1.7$; bursting phase difference variation with time for (b) $k_1 = 1.3$.

as shown in Fig. 11(a)(b). When $I = 2$ and the system is in perfect periodic-2 synchronization, the phase diagrams of $q = 0.56$ and $q = 0.9$ are as shown in Fig. 11(c)(d). Compared with the situation when $I = 3$, there are some differences. It can be inferred that under the influence of different external stimulus currents, the synchronization transition of the system changes.

From Fig. 11, when the system is in perfect synchronization, the neurons are in periodic bursting under the selected fractional-order, but the two neurons are in periodic-5 synchronization when $I = 3.5, q = 0.56$ and is in spiking synchronization when $I = 3.5, q = 0.9$. To further understand the effect of fractional-order changes on the firing model of coupled neurons under different external stimulation currents when the system is in perfect synchronization, the bifurcation diagrams of one neuron for ISI when $I = 3.5$, $I = 2$ and $I = 1.4$ are plotted in Fig. 12. As shown in Fig. 12(a), when $I = 3.5$ and $0.55 < q < 0.57$, the system is in periodic synchronization. Increasing the fractional-order, when $0.57 < q < 0.67$, two periodic windows appear around $q = 0.6$ and $q = 0.63$, while the system is in chaotic synchronization in other regions. When $0.67 < q < 1$, the system is in periodic synchronization. From Fig. 12(b)(c), the system is in periodic synchronization when $I = 2$ and $I = 1.4$.

In Fig. 13, the phase diagrams of $(z_{1,2}, x_{1,2})$ show the synchronization transition of the system in detail with fractional-order changes when $I = 3.5, k_1 = 3$, and the neurons are in perfect synchronization. As shown in Fig. 13(a), the system is in periodic synchronization and the neurons display periodic-5 bursting when $q = 0.55$. The system is in chaotic synchronization when $q = 0.56$(Fig. 13(b)). The system is in

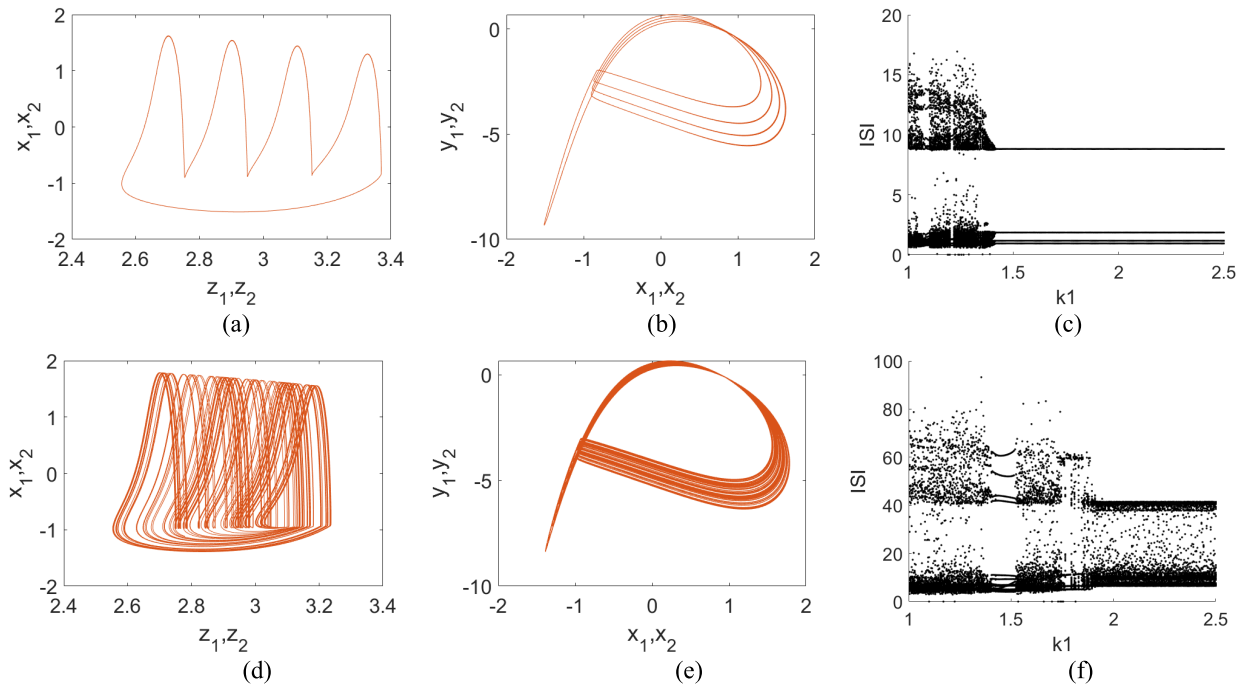

FIGURE 9. Phase diagrams of $(x_{1,2}, z_{1,2})$ for $k_1 = 3$: (a) $q = 0.56$, and (d) $q = 0.9$. Phase diagrams of $(x_{1,2}, y_{1,2})$ for $k_1 = 3$: (a) $q = 0.56$, and (d) $q = 0.9$. ISI bifurcation diagrams for $k_1 = 3$: (a) $q = 0.56$, and (d) $q = 0.9$.

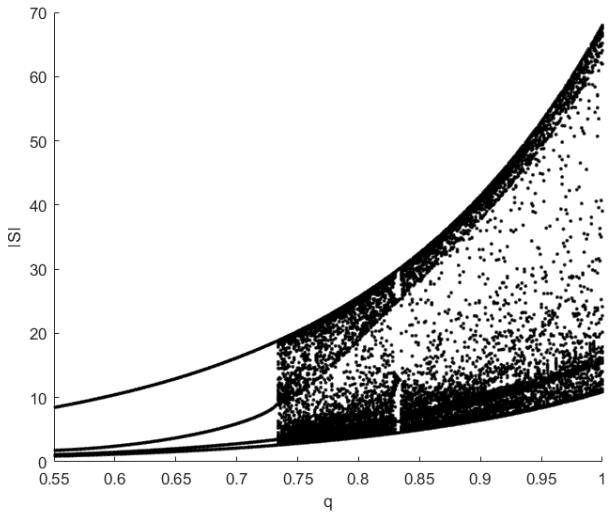

FIGURE 10. ISI bifurcation of the first neuron when $I = 3, k_1 = 3$.

periodic synchronization and the neurons display periodic-4, periodic-2 bursting and periodic spiking when $q = 0.58$, $q = 0.67$,$q = 0.7$, and $q = 0.85$ (Fig. 13(c)-(f)).

In conclusion, with a change in the fractional-order, the threshold of k_1 when the memristive synapse-coupled neuronal network enters perfect synchronization changes. Under different fractional-orders, the synchronization transition mode of coupled neurons differs with increasing k_1. At some fractional-orders, the synchronization transition of the system does not strictly follow the transition [21] from phase synchronization to perfect synchronization with increasing k_1, and perfect synchronization can occur before phase synchronization when the fractional-order is in the range [0.59, 0.64]. In addition, when $I = 3$, a change in the fractional-order leads to the transition between perfect periodic-4 synchronization and perfect chaotic synchronization. If the external stimulation current I changes, the effect of the fractional-order on the system synchronization mode also changes. In this paper, the effect of the fractional-order on the synchronization mode is analyzed by taking $I = 3.5$, $I = 2$, and $I = 1.4$ as examples. The simulation results show that no matter how the fractional-order changes, the system is in periodic synchronization when $I = 2$ and $I = 1.4$. When $I = 3.5$, a change in the fractional-order also leads to a transition between perfect periodic synchronization (perfect periodic-5 synchronization, perfect periodic-4 synchronization, perfect periodic-2 synchronization, or perfect spiking synchronization) and chaotic perfect synchronization, but the regions of chaotic synchronization and periodic synchronization are different from the regions when $I = 3$.

IV. SYNCHRONIZATION AND SPATIOTEMPORAL PATTERNS OF THE MEMRISTIVE SYNAPSE-COUPLED FRACTIONAL-ORDER NEURONAL RING NETWORK

In this section, we analyze the influences of the fractional-order on the synchronization of a coupled ring network, and the chimera state induced by the fractional-order.

A. DESCRIPTIONS OF THE STRENGTH OF INCOHERENCE AND THE SYNCHRONIZATION FACTOR

To depict the collective behaviors of the neuronal network, the strength of incoherence (SI) was proposed in [23].

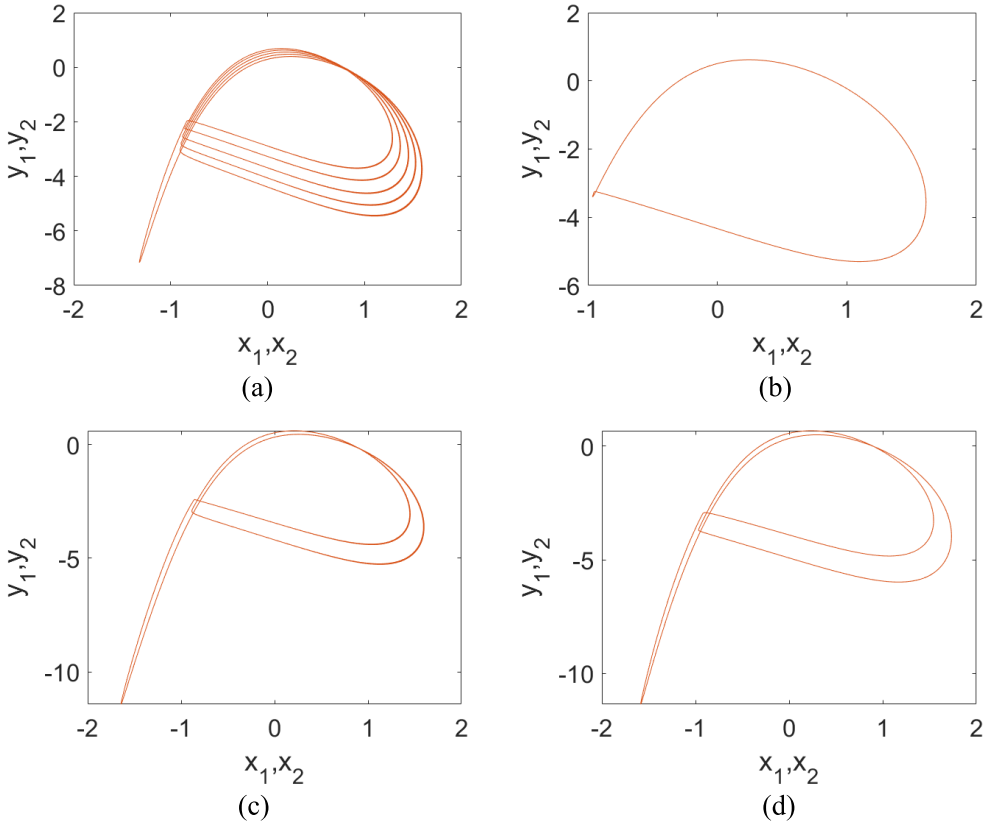

FIGURE 11. Phase diagram of $\left(y_{1,2}, x_{1,2}\right)$ for $k_1 = 3$ (a) $I = 3.5, q = 0.56$, (b) $I = 3.5, q = 0.9$, (c) $I = 2, q = 0.56$, and (d) $I = 2, q = 0.9$.

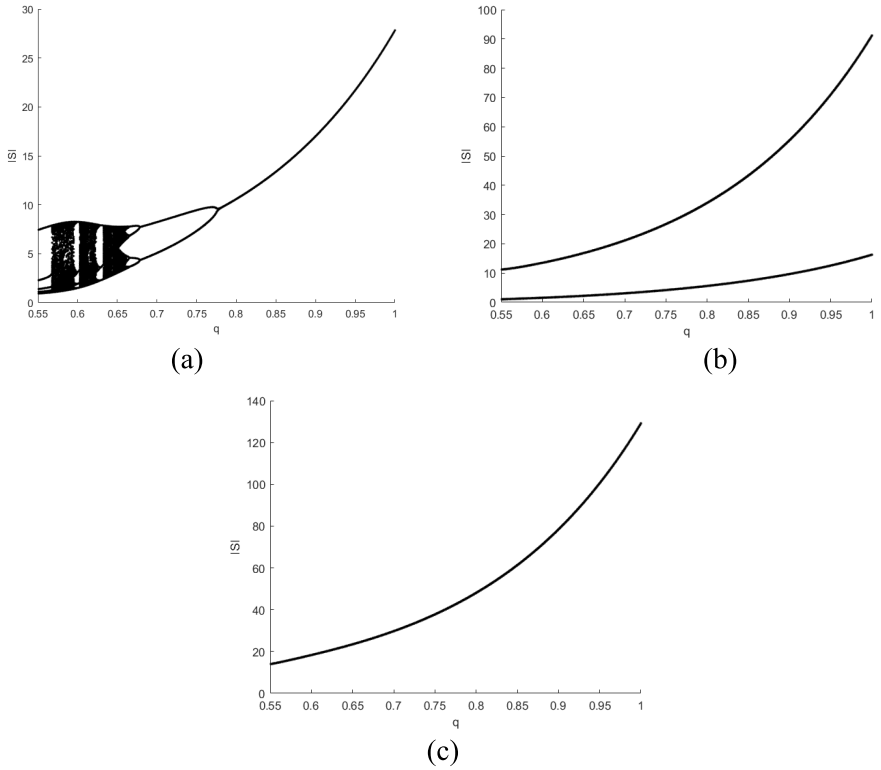

FIGURE 12. ISI bifurcation diagrams of the first neuron for $k_1 = 3$: (a) $I = 3.5$, (b) $I = 2$, and (c) $I = 1.4$.

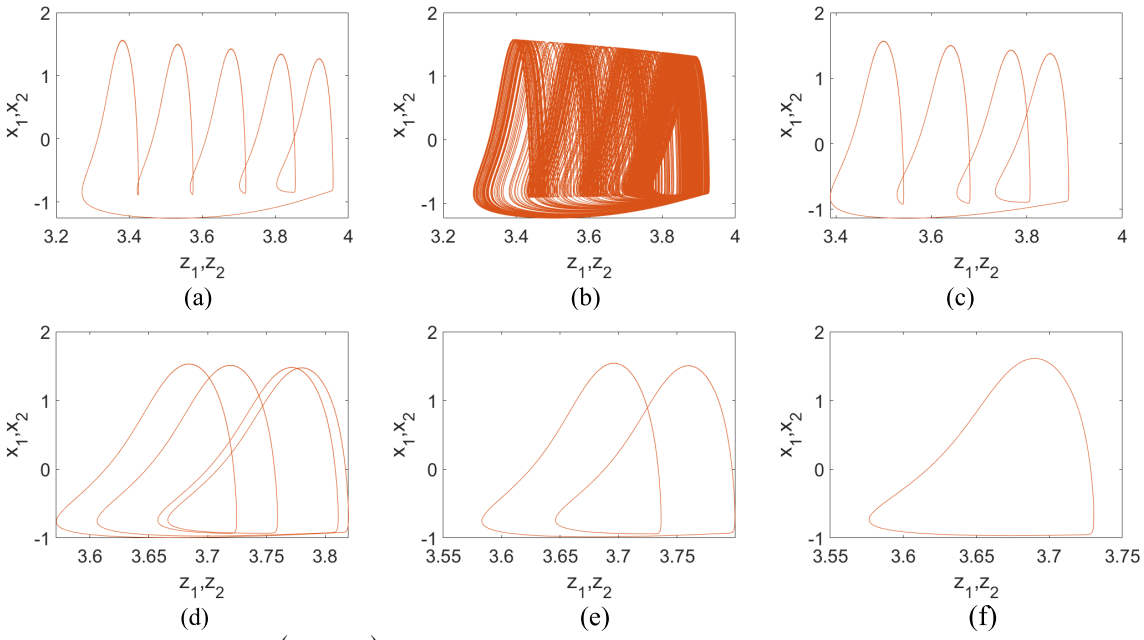

FIGURE 13. Phase diagrams of $(x_{1,2}, z_{1,2})$ for $I = 3.5, k_1 = 0.3$: (a) $q = 0.55$, (b) $q = 0.57$, (c) $q = 0.6$, (d) $q = 0.67$, (e) $q = 0.7$, and (f) $q = 0.85$.

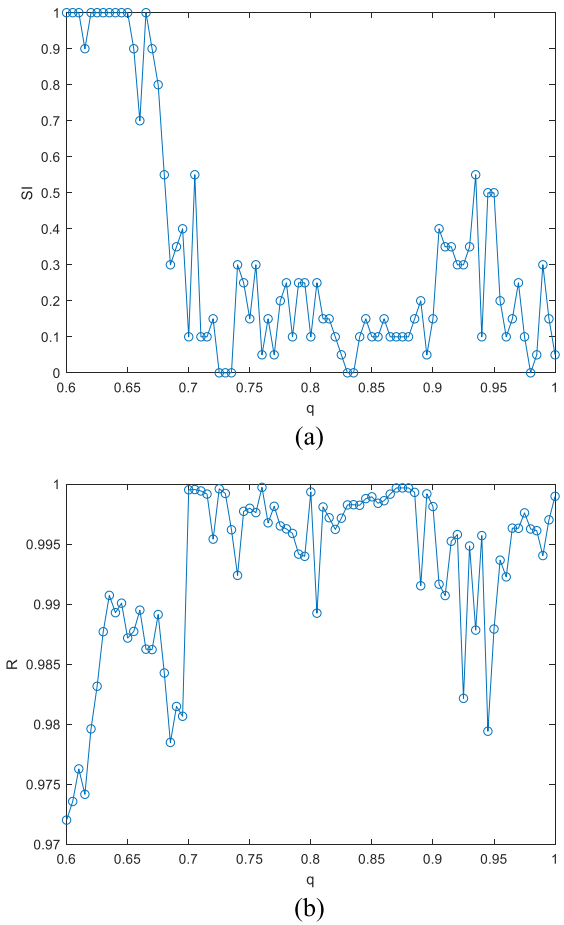

FIGURE 14. The curves of (a) $SI \sim q$, and (b) $R \sim q$.

The transformation variables are denoted $w_i = x_{1(i+1)} - x_{1i}$, and the number of neuronal subnetworks can be divided into M bins of equal length $n = {}^{N}/_{M}$. A local standard deviation is defined as

$$\sigma(m) = \sqrt{\frac{1}{n}\sum_{j=n(m-1)+1}^{mn}\left(w_j - \langle w\rangle\right)^2}$$

in which $m = 1, 2, \ldots, M$ is the mth bin, $w = \frac{1}{N}\sum_{i=1}^{N} w_i$, and $\langle\bullet\rangle_t$ stands for a temporal average. Thus, the SI can be calculated by

$$SI = 1 - \frac{\sum_{m=1}^{M}\Theta(\delta - \sigma(m))}{M} \tag{7}$$

where $\Theta(\bullet)$ and δ represent the Heaviside step function and a preset threshold, respectively. The resulting values SI = 1 and 0 indicate incoherent and coherent states, respectively, whereas $0 < \mathrm{SI} < 1$ corresponds to the chimera states.

The synchronization factor R can describe the synchronization of the network. R is given by

$$R = \frac{\langle F^2\rangle - \langle F\rangle^2}{\frac{1}{N}\sum_{i=1}^{N}\left(\langle x_i^2\rangle - \langle x_i\rangle^2\right)}, \quad F = \frac{1}{N}\sum_{i=1}^{N} x_i \tag{8}$$

where $\langle\cdot\rangle$ denotes temporal averaging. The value of R is between 0 and 1 and increases with decreasing average membrane potential errors. More precisely, perfect synchronization of the neuronal network is expected when R is close to 1, and a non-synchronization state may appear when R is close to 0.

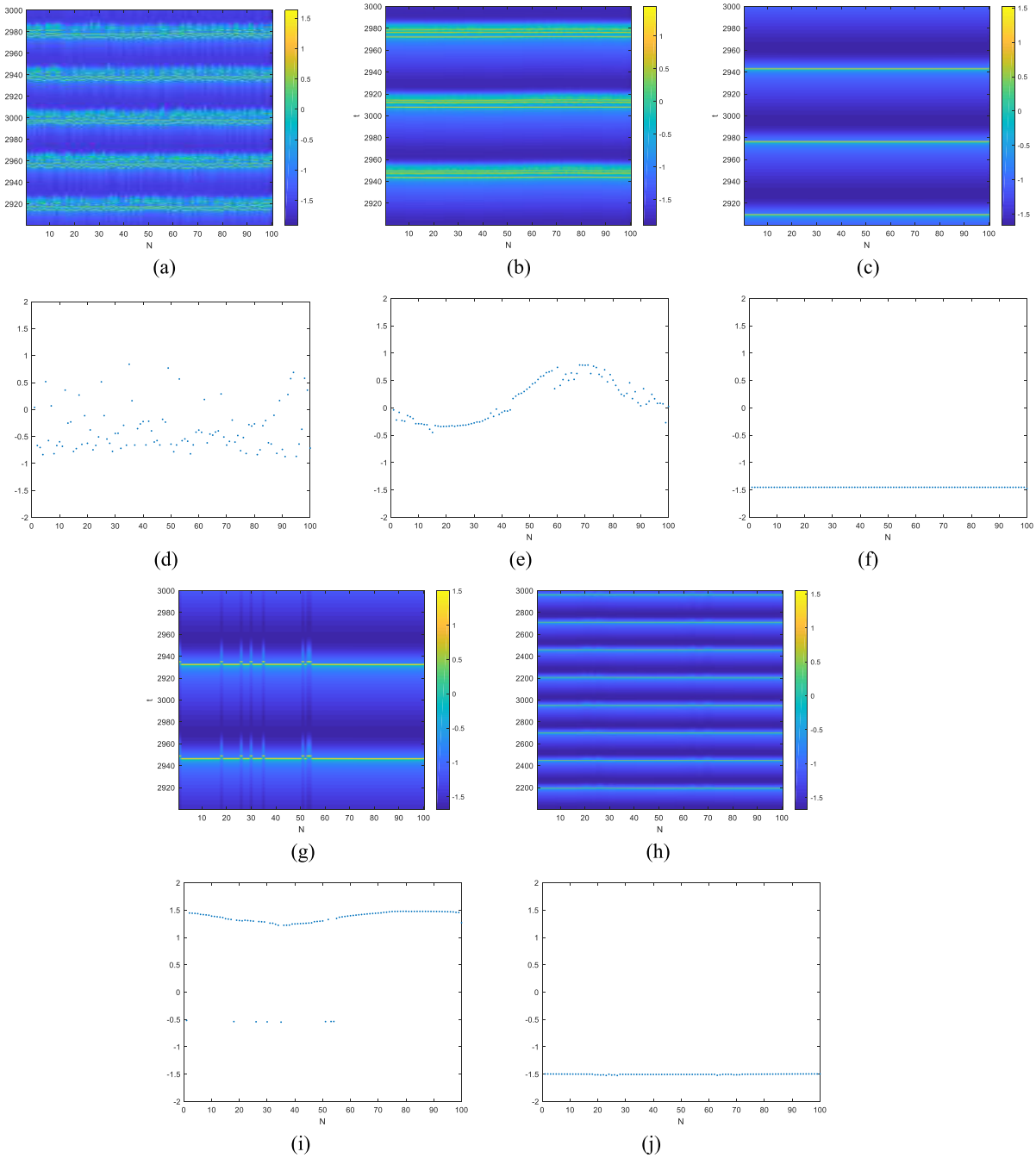

FIGURE 15. Neuronal network's spatiotemporal patterns and corresponding snapshots for (a)(b) $q = 0.6$, (c)(d) $q = 0.675$, (e)(f) $q = 0.725$, (g)(h) $q = 0.775$, and (i)(j) $q = 1$.

B. SYNCHRONIZATION AND SPATIOTEMPORAL PATTERNS UNDER THE INFLUENCE OF THE FRACTIONAL-ORDER

The coupling strength and parameter k_1 are fixed as $D = 0.8$, $k_1 = 1$, and the fractional-order is changing. The curves of $SI \sim q$ and $R \sim q$ are presented in Fig. 14. When the strength of the incoherence is 0, the neurons are in a coherent state, but the synchronization factor is inverted. From Fig. 14(a), when $0.6 < q < 0.615$ and $0.62 < q < 0.665$, SI = 1, and the ring network is in an incoherent state. The ring network then goes into the chimera state when $0.65 < q < 0.725$. Then, the coherent state appears at $q = 0.725$ and $q = 0.83$. A chimera state with $0 < \mathrm{SI} < 1$ appears when $0.75 < q < 0.83$ and $0.84 < q < 0.1$. From a synchronization point of view, as shown in Fig. 14(b) the ring network is in perfect synchronization at some fractional-orders but not in synchronization at some other fractional-orders.

To observe the incoherent, coherent, and chimera states when the fractional-order varies, the spatiotemporal patterns and corresponding snapshots of the ring network are shown

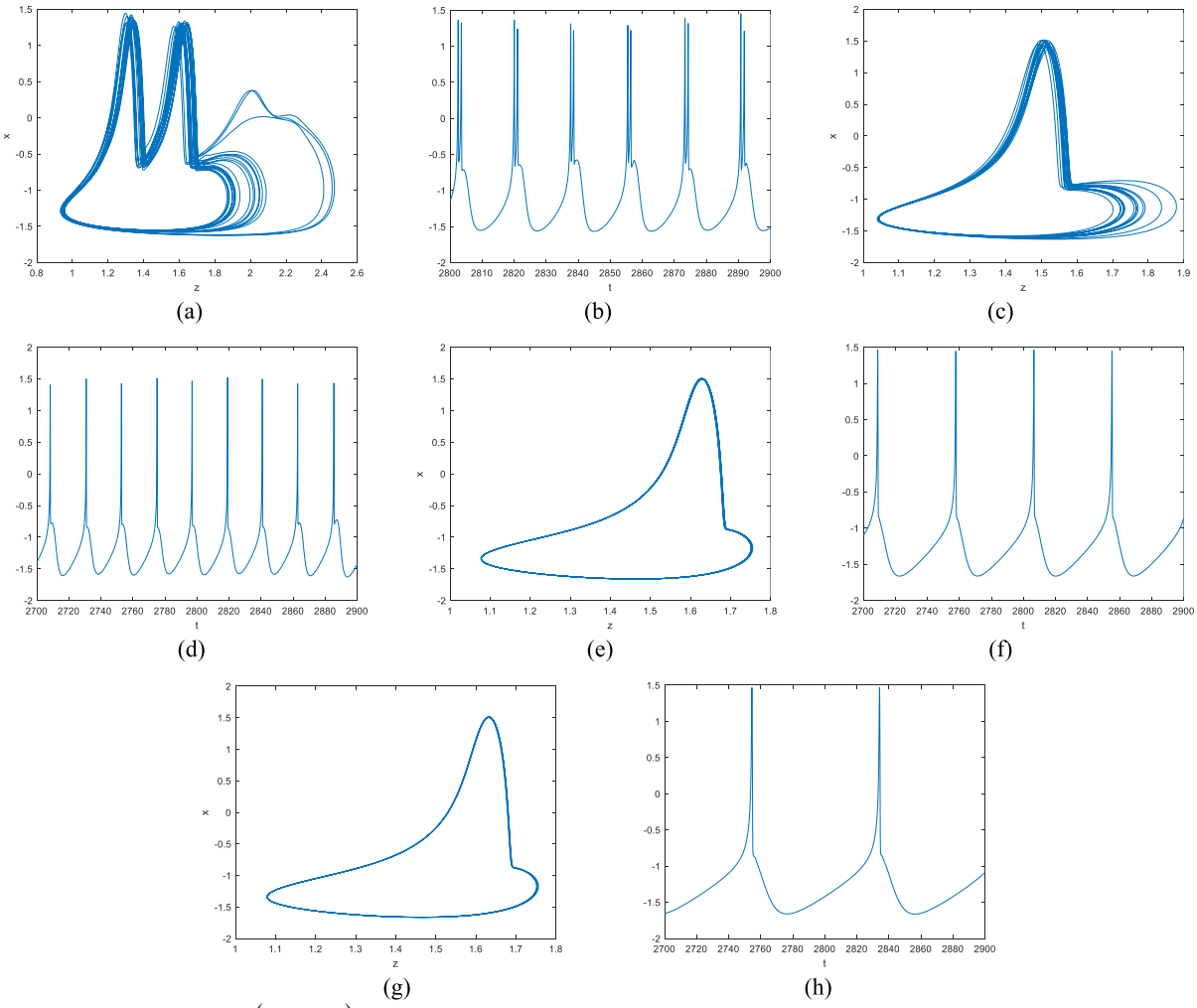

FIGURE 16. Phase diagram of $\left(x_{1,2}, z_{1,2}\right)$ (first panel) and the corresponding time series of x (second panel) for (a)(b) $q = 0.6$, (c)(d) $q = 0.64$, (e)(f) $q = 0.8$, and (g)(h) $q = 0.75$.

in Fig. 15. As shown in Fig. 15(a)(d), when $q = 0.6$, the network is in an incoherent state, because all x_{1i} are disorderly. When $q = 0.675$, the network is in a chimera state because the indices 1-10, 37-43, and 60-100 are incoherent with the other subnetworks, as shown in Fig.15(b)(e). As shown in Fig. 15(e)(f) and (i)(j), the network is in a coherent state and x_{1i} contains uniformly distributed values when $q = 0.725$ and $q = 1$. When $q = 0.775$,the network is in a chimera state because the indices 1, 18, 30, 35 and 51-54 are disorderly.

It can be concluded from the above analysis that the collective behaviors of the neuronal network change if the fractional-order changes. A change in the fractional-order induces the synchronization to become asynchronized. The fractional-order can induce an incoherent state, chimera state and coherent state. In addition, the transitions between the collective behaviors are complex. Therefore, the fractional-order is also an important parameter that can change the collective behaviors of the neuronal network.

To determine the synchronization transition of the neuronal network, k_1 is set as 2, so the network is in perfect synchronization. The corresponding time series of x_{1i} and the phase diagrams of (z_{1i}, x_{1i}) are plotted in Fig. 16. When the fractional-order is small, the neurons in the network display bursting, but the neurons display spiking for other fractional-orders. As shown in Fig. 16(a)(b), when $q = 0.6$, the neurons display bursting, and there are two spikes. When $q = 0.64$, the neurons display spiking, as shown in Fig. 16(c)(d), As shown in Fig. 16(e)-(h), the neurons of the network display periodic spiking when $q = 0.8$ and $q = 0.75$.

In conclusion, when the coupling strength and k_1 are fixed, different fractional-orders can induce different collective behaviors, such as the coherent, incoherent and chimera states. The neuronal network is in perfect synchronization at some fractional-orders. Synchronization transitions can also be induced by the fractional-order because the firing modes of neurons in the network can be changed by the fractional-order.

V. CONCLUSION

This paper focuses on the synchronization collective behaviors and synchronization transitions of memristive synapse-coupled fractional-order neuronal networks. First, a

fractional-order HR model coupled with memristive synapses and ring network coupled subnetworks are constructed. Then, the synchronization and synchronization transition of two memristive synapse-coupled fractional-order neurons are investigated by using the similarity function, phase difference and numerical simulation. Finally, the synchronization and spatiotemporal patterns of the ring network coupled with subnetworks are studied by the SI and the synchronization factor. For the two memristive synapse-coupled neurons, the results show that the fractional-order can change the threshold of k_1 when the system is in perfect synchronization. In [21], the two coupled neurons' degree of synchronization was found to increase with increasing k_1. However, in this paper, an exception can be found when the fractional-order is in the range $[0.59, 0.64]$; the numerical results show that some fractional-orders can induce perfect synchronization before phase synchronization. At different fractional-orders, the firing mode of the system changes when the system is in synchronization. When $I = 3$ and the two neurons are in perfect synchronization, the fractional-order can induce a synchronization transition of perfect periodic synchronization (periodic-4 synchronization) and perfect chaotic synchronization. In addition, for different I, the effect of the fractional-order is different. When $I = 3.5$, the fractional-order can also induce a synchronization transition of perfect periodic synchronization (periodic-5,4,2 synchronization and spiking synchronization) and chaotic synchronization. When $I = 2, 1.4$, the two neurons are only in perfect periodic-2 synchronization for all fractional-orders in $[0.55, 1]$. For the ring network coupled subnetworks, the result of the numerical simulation shows that the fractional-order can induce a coherent state, an incoherent state and a chimera state. In other words, the network is in perfect synchronization at some fractional-orders but asynchronized in some other fractional-orders. The fractional-order can induce the synchronization transition because the firing model is different. In short, the fractional-order is an important parameter that can induce different synchronization behaviors of neuronal networks, and memristive synapse-coupling can make the synchronization behaviors more complex.

REFERENCES

[1] A. L. Hodgkin and A. F. Huxley, "A quantitative description of membrane current and its application to conduction and excitation in nerve," *J. Physiol.*, vol. 117, no. 4, pp. 500–544, 1952.

[2] R. FitzHugh, "Impulses and physiological states in theoretical models of nerve membrane," *Biophys. J.*, vol. 1, no. 6, pp. 445–466, 1961.

[3] C. Morris and H. Lecar, "Voltage oscillations in the barnacle giant muscle fiber," *Biophys. J.*, vol. 35, no. 1, pp. 193–213, Jul. 1981.

[4] A. Bandyopadhyay and S. Kar, "Impact of network structure on synchronization of Hindmarsh–Rose neurons coupled in structured network," *Appl. Math. Comput.*, vol. 333, pp. 194–212, Sep. 2018.

[5] F. Parastesh, C.-Y. Chen, H. Azarnoush, S. Jafari, and B. Hatef, "Synchronization patterns in a blinking multilayer neuronal network," *Eur. Phys. J. Special Topics*, vol. 228, no. 11, pp. 2465–2474, Oct. 2019.

[6] R. C. Budzinski, B. R. R. Boaretto, T. L. Prado, R. L. Viana, and S. R. Lopes, "Synchronous patterns and intermittency in a network induced by the rewiring of connections and coupling," *Chaos, Interdiscipl. J. Nonlinear Sci.*, vol. 29, no. 12, Dec. 2019, Art. no. 123132.

[7] Q. Wang, Z. Duan, M. Perc, and G. Chen, "Synchronization transitions on small-world neuronal networks: Effects of information transmission delay and rewiring probability," *EPL Europhys. Lett.*, vol. 83, no. 5, Sep. 2008, Art. no. 50008.

[8] T. Pérez, G. C. Garcia, V. M. Eguíluz, R. Vicente, G. Pipa, and C. Mirasso, "Effect of the topology and delayed interactions in neuronal networks synchronization," *PLoS ONE*, vol. 6, no. 5, May 2011, Art. no. e19900.

[9] X. Sun, M. Perc, and J. Kurths, "Effects of partial time delays on phase synchronization in Watts–Strogatz small-world neuronal networks," *Chaos, Interdiscipl. J. Nonlinear Sci.*, vol. 27, no. 5, May 2017, Art. no. 053113.

[10] Y. Wang, X. Shi, B. Cheng, and J. Chen, "Synchronization and rhythm transition in a complex neuronal network," *IEEE Access*, vol. 8, pp. 102436–102448, 2020.

[11] M. M. Ibrahim and I. H. Jung, "Complex synchronization of a ring-structured network of FitzHugh–Nagumo neurons with single-and dual-state gap junctions under ionic gates and external electrical disturbance," *IEEE Access*, vol. 7, pp. 57894–57906, 2019.

[12] P. Ge and H. Cao, "Synchronization of Rulkov neuron networks coupled by excitatory and inhibitory chemical synapses," *Chaos, Interdiscipl. J. Nonlinear Sci.*, vol. 29, no. 2, Feb. 2019, Art. no. 023129.

[13] D. Wang, Y. Sun, F. Wang, and J. Li, "Modeling oscillatory phase and phase synchronization with neuronal excitation and input strength in cortical network," *IEEE Access*, vol. 6, pp. 36441–36458, 2018.

[14] J. C. Shi, M. Luo, and C. S. Huang, "Dependence of synchronization transitions on mean field approach in two-way coupled neural system," *Indian J. Phys.*, vol. 92, no. 8, pp. 1009–1016, Aug. 2018.

[15] M. Ge, Y. Jia, J. B. Kirunda, Y. Xu, J. Shen, L. Lu, Y. Liu, Q. Pei, X. Zhan, and L. Yang, "Propagation of firing rate by synchronization in a feed-forward multilayer Hindmarsh–Rose neural network," *Neurocomputing*, vol. 320, pp. 60–68, Dec. 2018.

[16] J. Ma, L. Mi, P. Zhou, Y. Xu, and T. Hayat, "Phase synchronization between two neurons induced by coupling of electromagnetic field," *Appl. Math. Comput.*, vol. 307, pp. 321–328, Aug. 2017.

[17] Y. Xu, Y. Jia, J. Ma, A. Alsaedi, and B. Ahmad, "Synchronization between neurons coupled by memristor," *Chaos Soliton. Fract.*, vol. 104, pp. 435–442, Nov. 2017.

[18] Q. Li, S. Tang, H. Zeng, and T. Zhou, "On hyperchaos in a small memristive neural network," *Nonlinear Dyn.*, vol. 78, no. 2, pp. 1087–1099, Oct. 2014.

[19] B. Bao, H. Qian, Q. Xu, M. Chen, J. Wang, and Y. Yu, "Coexisting behaviors of asymmetric attractors in hyperbolic-type memristor based Hopfield neural network," *Frontiers Comput. Neurosci.*, vol. 11, p. 81, Aug. 2017.

[20] H. Bao, Y. Zhang, W. Liu, and B. Bao, "Memristor synapse-coupled memristive neuron network: Synchronization transition and occurrence of chimera," *Nonlinear Dyn.*, vol. 100, no. 1, pp. 937–950, Mar. 2020.

[21] Q. Zhou and D. Wei, "Synchronous dynamics in multilayer memristive neural networks: Effect of electromagnetic induction," *IEEE Access*, vol. 8, pp. 164727–164736, 2020.

[22] F. Xu, J. Zhang, M. Jin, S. Huang, and T. Fang, "Chimera states and synchronization behavior in multilayer memristive neural networks," *Nonlinear Dyn.*, vol. 94, no. 2, pp. 775–783, Oct. 2018.

[23] Z. Wang, X. Huang, and G. Shi, "Analysis of nonlinear dynamics and chaos in a fractional order financial system with time delay," *Comput. Math. Appl.*, vol. 62, no. 3, pp. 1531–1539, 2011.

[24] Y. Fu, Y. Kang, and G. Chen, "Stochastic resonance based visual perception using spiking neural networks," *Frontiers Comput. Neurosci.*, vol. 14, p. 24, May 2020.

[25] T. J. Anastasio, "The fractional-order dynamics of brainstem vestibulo-oculomotor neurons," *Biol. Cybern.*, vol. 72, no. 1, pp. 69–79, Nov. 1994.

[26] K. Rajagopal, N. Hasanzadeh, F. Parastesh, I. I. Hamarash, S. Jafari, and I. Hussain, "A fractional-order model for the novel coronavirus (COVID-19) outbreak," *Nonlinear Dyn.*, vol. 101, no. 1, pp. 711–718, Jul. 2020.

[27] J. E. Solís-Pérez, J. F. Gómez-Aguilar, D. Baleanu, F. Tchier, and L. Ragoub, "Anti-synchronization of chaotic systems using a fractional conformable derivative with power law," *Math. Methods Appl. Sci.*, vol. 44, no. 10, pp. 8286–8301, Jul. 2021.

[28] D. Jun, Z. Guang-jun, X. Yong, Y. Hong, and W. Jue, "Dynamic behavior analysis of fractional-order Hindmarsh–Rose neuronal model," *Cognit. Neurodyn.*, vol. 8, no. 2, pp. 167–175, Apr. 2014.

[29] T. A. Giresse, K. T. Crepin, and T. Martin, "Generalized synchronization of the extended Hindmarsh–Rose neuronal model with fractional order derivative," *Chaos Soliton. Fract.*, vol. 118, pp. 311–319, Jan. 2019.

[30] F. Meng, X. Zeng, Z. Wang, and X. Wang, "Adaptive synchronization of fractional-order coupled neurons under electromagnetic radiation," *Int. J. Bifurcation Chaos*, vol. 30, no. 3, Mar. 2020, Art. no. 2050044.
[31] F. Meng, X. Zeng, and Z. Wang, "Dynamical behavior and synchronization in time-delay fractional-order coupled neurons under electromagnetic radiation," *Nonlinear Dyn.*, vol. 95, no. 2, pp. 1615–1625, Jan. 2019.
[32] R. Li, *Chaotic Synchronization of a Class of Fractional-Order System*. Xi'an, China: Air Force Engineering Univ., 2014.
[33] S. Majhi, M. Perc, and D. Ghosh, "Chimera states in uncoupled neurons induced by a multilayer structure," *Sci. Rep.*, vol. 6, no. 1, Dec. 2016, Art. no. 39033.
[34] S. Rakshit, B. K. Bera, M. Perc, and D. Ghosh, "Basin stability for chimera states," *Sci. Rep.*, vol. 7, no. 1, p. 2412, May 2017.
[35] R. Gopal, V. K. Chandrasekar, A. Venkatesan, and M. Lakshmanan, "Observation and characterization of chimera states in coupled dynamical systems with nonlocal coupling," *Phys. Rev. E, Stat. Phys. Plasmas Fluids Relat. Interdiscip. Top.*, vol. 89, no. 5, May 2014, Art. no. 052914.
[36] F. Parastesh, S. Jafari, H. Azarnoush, B. Hatef, H. Namazi, and D. Dudkowski, "Chimera in a network of memristor-based Hopfield neural network," *Eur. Phys. J. Special Topics*, vol. 228, no. 10, pp. 2023–2033, Oct. 2019.
[37] D. Dudkowski, K. Czołczyński, and T. Kapitaniak, "Traveling chimera states for coupled pendula," *Nonlinear Dyn.*, vol. 95, no. 3, pp. 1859–1866, Feb. 2019.
[38] T. Fang, J. Zhang, S. Huang, F. Xu, M. Wang, and H. Yang, "Synchronous behavior among different regions of the neural system induced by electromagnetic radiation," *Nonlinear Dyn.*, vol. 98, no. 2, pp. 1267–1274, Oct. 2019.
[39] K. Diethelm, N. J. Ford, and A. D. Freed, "A predictor-corrector approach for the numerical solution of fractional differential equations," *Nonlinear Dyn.*, vol. 29, nos. 1–4, pp. 3–22, 2002.
[40] S. Bhalekar, V. Daftardar-Gejji, D. Baleanu, and R. Magin, "Fractional Bloch equation with delay," *Comput. Math. Appl.*, vol. 61, no. 5, pp. 1355–1365, Mar. 2011.
[41] H. Shao-Bo, S. Ke-Hui, and W. Hui-Hai, "Solution of the fractional-order chaotic system based on Adomian decomposition algorithm and its complexity analysis," *Acta Phys. Sinica*, vol. 63, no. 3, 2014, Art. no. 030502.
[42] H. Wu, X. Zhang, S. Xue, L. Wang, and Y. Wang, "LMI conditions to global Mittag–Leffler stability of fractional-order neural networks with impulses," *Neurocomputing*, vol. 193, pp. 148–154, Jun. 2016.
[43] I. Podlubny, *Fractional Differential Equations*. New York, NY, USA: Academic, 1999.
[44] F. Wang, Y. Yang, A. Hu, and X. Xu, "Exponential synchronization of fractional-order complex networks via pinning impulsive control," *Nonlinear Dyn.*, vol. 82, no. 4, pp. 1979–1987, Dec. 2015.

YANG XIN received the B.S. degree in information and computing science from Air Force Engineering University, Xi'an, China, in 2019, where he is currently pursuing the M.S. degree in control science and engineering. His research interests include nonlinear dynamics, neuronal networks, stochastic resonance, and synchronization transition.

ZHANG GUANGJUN received the B.S. and M.S. degrees from Air Force Engineering University, China, and the Ph.D. degree from Xi'an Jiaotong University, China. He is currently a Professor with Air Force Engineering University. He has published over 80 scientific articles in refereed journals and proceedings. His research interests include nonlinear dynamics and control, chaos, and resonance and control of nonlinear dynamics.